AUTOMATIC INTENSITY QUANTIFICATION OF FLUORESCENCE TARGETS FROM MICROSCOPE IMAGES WITH MAXIMUM LIKELIHOOD ESTIMATION

Harri Pölönen, Jussi Tohka and Ulla Ruotsalainen

Department of Signal Processing, Tampere University of Technology
Korkeakoulunkatu 10, 33720 Tampere, Finland
phone: + (358) 3 3115 3912, fax: + (358) 3 3115 2929
web: www.cs.tut.fi/sgn/m2obsi

ABSTRACT

We introduce a method to determine the quantitative intensity values and sub-pixel locations of closely located small targets from noisy fluorescence microscope images. We model the microscope image with a mixture of point spread functions and the image noise with a stochastic process containing Poisson distribution. Maximum likelihood estimation is used to find the optimal parameters for the model. Numerical ML estimation is performed with differential evolution optimization algorithm. To evaluate the methods, noisy simulated images were created with closely located targets. Methods were compared to conventional methods based on low-pass filtering and Gaussian mixture fitting, and the simulations show better accuracy for the new method. A real microscope image is also quantified to show that the model is applicable in practice.

1. INTRODUCTION

Fluorescence microscopy is used to examine various biological structures such as plasma membrane of a living cell. Target of interest is labelled with a fluorescent tag and excited with a powerful light source of specific wavelength. When the excitation state of a fluorophore is released, photons are emitted. Due to energy loss during the excitation state, the emission wavelength is slightly longer than the excitation wavelength and they can be separated from each other with a filter (e.g. stained glass). The emission light is then detected with a digital CCD camera and a digital image of locations and quantities of excitated fluorophores is formed.

By determining the locations and intensities of fluorescent targets, the properties of the specimen (e.g. cell membrane) can be analysed. The information contained in the acquired image is constrained not only by the sampling frequency (image resolution) of the camera but also by the optical diffraction limit of the microscope system and image noise. The optical resolution is dependent on the numerical aperture of the used lens and the emitted light wavelength of the fluorophore. Both the light wavelength and the numerical aperture are limited, and thus the optical resolution is limited as well.

Due to limited optical resolution sub-resolution fluorescent targets, i.e. fluorescent concentrations smaller than the image pixel size, appear as spots in the image covering several pixels wider area than the corresponding true fluorescent target. These spots are commonly quantified by smoothing the image with a low-pass filter and fitting a Gaussian mixture model to the filtered image (e.g. in [1] and [9]). The motivation in such approaches is to exclude the high-frequency noise component, but inevitably also a portion of the quantitative information is lost in the process. The smoothed image is usually more appealing to the human eye, but automatic quantification would be more accurate if performed on the raw image. In addition, the Gaussian surface is not the true shape produced by the subresolution target but merely an approximation (see [2]). The weaknesses in the conventional method are most crucial in cases, where two or more targets are located close to each other. Targets closer than the Rayleigh limit appear as a single spot in the image and the individual sub-pixel locations and quantitative intensities of targets within these clusters are challenging to determine.

In this study, we describe a new method to overcome the inaccuracies caused by the above mentioned issues by modelling the raw microscope image with a stochastic model and using maximum likelihood estimation to determine the optimal model parameters. We model a fluorescent target with an appropriate point spread function, which can be calculated accordind to the microscope settings. Targets, which are located close to each other, are modelled with a mixture of point spread functions. The noise in a microscope image is modelled as a process related to Poisson distribution. The noise strength and the background level of the image are estimated in the ML optimization process. Because the noise magnitude is estimated, the noise throughout the image can be utilized to obtain more accurate parameter estimates. The multimodal numerical estimation is performed with differential evolution search algorithm, to find the global optimum of ML criterion.

Noisy simulated images with closely located targets were created to evaluate the developed method with the conventional ones. An application to cell membrane caveolae quantification is presented to test the capability to cope with a real microscope image.

2. METHODS

2.1 Model description

The microscope image is a transformed and noisy representation of the true distribution of fluorophores. The transformation is determined by the point-spread function (PSF) of the microscope and is commonly modelled as a convolution between the PSF and the true distribution of fluorophores. The image noise is assumed to be a Poisson type process, which contains several acquisition error sources such as shot noise. [4]

In this paper we consider only fluorescent targets smaller than the diffraction limit of the microscope, and thereby all the targets appear in the transformed image as spots shaped

© EURASIP, 2009

as the point spread function of the microscope. As in [3, 9] we define the PSF as

$$P(r) = \left(\frac{2J_1(ra)}{r} \right)^2 \qquad \text{with} \qquad a = \frac{2\pi A}{\lambda} \tag{1}$$

where r is the distance from the centroid, J_1 is the Bessel function of first kind, A stands for the numerical aperture of the used solvent (e.g. water, oil) and λ for the emission wavelength of the used fluorophore. The equation is not properly defined in case of $r = 0$, and the limit

$$\lim_{r \to 0} P(r)$$

is then used instead.

A spot in the noise-free image model is formed by determining the spot pixel intensities according to the distance from the pixel centre to the true centre of the corresponding target. If we denote the true centre point of a target n as (t_x^n, t_y^n) and the intensity (brightness) of this target as t_α^n, the pixel intensity at location (x,y) due to spot n is

$$S^n(x,y) = t_\alpha^n P(\sqrt{(t_x^n - x)^2 + (t_y^n - y)^2}),$$

where P is the point spread function in Equation (1). Note that the true target locations t_x and t_y are not bound to pixel coordinates, but can have any value in the limits of numerical accuracy. A sub-pixel accuracy for the locations can thereby be achieved. In addition, we include a background intensity β in the image model, representing the background autofluorescence. Because we study quite small areas of the image at a time, we assume that background is constant within that region. Thus, the model for the pixel intensity of the noise-free image $C(x,y)$ at pixel location (x,y) becomes

$$C(x,y) = \beta + \sum_n S^n(x,y).$$

We assume that the shot noise is dominating the other error sources and the microscope image is thus contaminated by Poisson type noise[2, 4]. We form a stochastic model for the image by assuming that the image pixel intensities are realizations of a certain stochastic process related to Poisson distribution of parameter λ dependent on square root of the noise-free pixel intensity $C(x,y)$. Because the true image noise is never a pure Poisson process (with variance equal to mean), we include a noise magnitude factor ρ, and the stochastic process at pixel (x,y) is stated as

$$N(x,y) \sim Poiss\left(\rho\sqrt{C(x,y)}\right) - \sqrt{C(x,y)}\left(\rho - \sqrt{C(x,y)}\right).$$

The mean of $N(x,y)$ is thus $\sqrt{C(x,y)}$ and the variance $\rho\sqrt{C(x,y)}$.

Now, we can search for the most likely model parameters

$$\theta = \{t_x^1, \ldots, t_x^n, t_y^1, \ldots, t_y^n, t_\alpha^1, \ldots, t_\alpha^n, \beta, \rho\}$$

for the observed image I through the Poisson probability function

$$p(\Omega|\lambda) = \frac{\lambda^\Omega e^{-\lambda}}{\Omega!}$$

by setting

$$\lambda(x,y) = \rho\sqrt{C(x,y)}$$

and

$$\Omega(x,y) = I(x,y) + \sqrt{C(x,y)}(\rho - \sqrt{C(x,y)}).$$

In practice, in order to get numerically useful likelihood values for a model, we maximize the sum of the logarithms of the pixel-wise likelihoods

$$f(\theta) = \sum_x \sum_y \log p(\Omega(x,y)|\lambda(x,y)). \tag{2}$$

The ML estimate $\hat{\theta}$ is then defined as

$$\hat{\theta} = \arg\max_\theta f(\theta).$$

2.2 Implementation

The overlapping spots generated by closely located targets, are the most challenging to quantify and we concentrate on these cases instead of single, separate spots. The whole image is divided into regions so that each region contains one group of (two or more) mutually overlapping spots, and each region is quantified separately. The noise magnitude multiplier ρ and the background intensity β are assumed to be constant within a region, but vary from region to another. A separate model with its unique parameters is searched for each region.

In practice spot detection is a major problem, i.e. determining the number of spots within a group of overlapping spots. In this study, however, we concentrate on the quantification of spot intensity and location and omit spot detection related issues. Therefore the correct number of spots is assumed to be known in simulations. With real microscope data the spots are detected by finding the local intensity maxima from low-pass filtered image as in [5]. The number of overlapping spots within a group was determined according to the group area. This simple spot detection method turned out to be sufficient to show the model applicability with real microscope images.

Due to the large number of simulations, we performed the estimations on a computer grid. On average we had about 400 modern computer cores in use and distributed each estimation problem, i.e. finding a model for a group of overlapping spots, to an individual core. This way the calculations could be performed with reasonable time cost.

2.3 Differential evolution algorithm

In previous experiments we found out that commonly used local estimation algorithms such as Levenberg-Marquardt were unable to find the global optimum for the problem, probably due to the multimodal nature of the estimation problem. Therefore a stochastic search algorithm is used to find the optimum parameters.

Differential evolution (DE) is a global stochastic optimization method which is closely related to genetic algorithms (GA)[7, 8]. DE is population-based, but unlike GA, the DE population is improved one member at a time instead of creating whole generations at once. In differential evolution a new parameter vector θ_C is constructed by subtracting the difference of two randomly chosen parameter vectors, say

θ_2 and θ_3, from another randomly chosen parameter vector θ_1. The formula can be written as

$$\theta_c = \theta_1 + K \cdot (\theta_2 - \theta_3), \quad (3)$$

where $K \in$R is the weight for the subtracted difference. Weight K can be seen also as a mutation length applied to the parameter vector θ_1. If the likelihood of the new parameter vector θ_C is better than the likelihood of yet another randomly chosen parameter vector θ_4, the population is updated by replacing θ_4 with θ_C. This cycle is repeated until the stopping criteria are met.

In this study we set the convergence rate parameter K random, so that in each θ_c creation a new value for K is randomly drawn from a unifrom distribution on the interval $]0,2]$. This removes the risk of stagnation (see [6]) of the estimation process because a different θ_c is created each time even with the same building components $\theta_1, \theta_2, \theta_3$ in equation (3). Although the risk of stagnation is small with large populations, it is worth avoiding in an automatic method such as this. Additionally, varying K makes the algorithm both explorative and exploitative, being able to search the parameter space widely but also converge once in a while. We also omitted the commonly used crossover operation from the algorithm as it turned out to have no significant effect on finding the global optimum.

The algorithm was run until the difference between the best and worst likelihood values of the population was numerically negligible (a threshold 10^{-6} was used). Then the algorithm was run again with a re-initialized population which included the best parameter vector achieved in the previous run. These reruns were performed until two consecutive runs produced the same results. The rerun cycle was included in the process for the sake of automaticity and robustness, although in vast majority of the experiments the second run didn't offer any improvements to the best parameter vector.

We used population size $50 + 20n$, where n is the number of components in the model i.e. the number of individual point spread functions in the mixture model. Our empirical tests showed that this population size was more than enough to avoid the local optima and keeps the time cost still reasonable (a few minutes per a group of overlapping spots). Initial population was created by choosing random values for the parameters from valid intervals. Locations (t_x, t_y) were initialized to be inside the image region, spot intensities (t_α) and background (β) level were initialized between zero and the sum of the region pixel values. The upper limit for the noise strength ρ was initially 10, which has been experimentally found to be sufficient. During the optimization the parameters were constrained only to positive values.

2.4 Reference methods

As a reference method we chose to use Gaussian mixture fitting to low-pass filtered image. Here we use two variations of this approach to evaluate the developed new model.

REF A. The first reference method is described in [9]. In this approach the shape of the Gaussian components is fixed, which leads to easier fitting with less parameters. The shape of the Gaussian components was determined according to microscope settings by setting the diagonal elements of the covariance matrix as

$$\sigma_{xy} = 0.21\frac{\lambda}{A} \quad (nm^2).$$

The raw microscope image was filtered with a matched kernel, i.e. the filtering kernel was exactly the same shape as the Gaussian components in the model. Originally, this method was developed for 3D case, but it is directly applicable to the 2D images. To find the parameter values, we used a nonlinear least squares fitting as in [9].

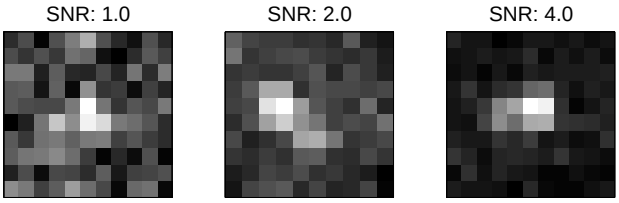

Figure 1: Overlapping pairs of simulated spots with different signal-to-noise ratios(SNR).

REF B. Another reference method in this study was fitting Gaussian mixture with free parameters to the filtered image as in [2]. We used again nonlinear least squares fitting to find the free parameters which are mean, covariance matrix and intensity of each Gaussian component. Furthermore, we defined the shape of Gaussians to be fairly symmetric. This was done by limiting the values of diagonal elements of covariance matrix within 20 % from each other. Also background level was included as an estimable parameter in the model to give more flexibility. We used a symmetric filter with Gaussian kernel variance $\sigma = 1$ to reduce the noise from the images.

3. EXPERIMENTS

3.1 Simulated data

We created simulated noisy images to evaluate the spot quantification methods. Two equally bright sub-resolution targets were placed to have a mutual distance of corresponding Rayleigh limit, the image was convolved with the appropriate point spread function and a background was added. To simulate the shot noise, a value for each pixel was randomly drawn from a Poisson distribution with parameter λ equal to the pixel intensity multiplied by noise factor ρ. The noise multiplier ρ was set separately with each image to produce a specific signal-to-noise ratio to the image. Signal-to-noise ratio is here defined as the mean intensity of the spot (brightest pixels) divided by the average noise deviation. Examples of simulated spots can be seen in Figure 1 with different signal-to-noise ratios. Six images were created with different signal-to-noise ratios and each image contained 1000 pairs of overlapping spots.

3.2 Simulation results

The simulated images were quantified with the developed method and the previously mentioned reference methods, and the results can be seen in Tables 1 and 2. The percentual intensity error (Table 1) is obtained by first calculating the absolute difference between the true intensity and

the estimated intensity, and then dividing it with the true intensity. The location error (Table 2) is the distance (norm) between the true location and the estimated location of each spot. Both tables show average values of errors within each image.

The most accurate results in both intensity and location estimation were achieved with the developed method when the signal-to-noise ratio is 1.5 or higher. Especially the intensity could be estimated with the developed method more accurately. The reference method B performed poorly in all simulations. The almost equal results for intensity estimates with Ref A regardless of the SNR can be explained by the fact that the filtering averages most of the Poisson noise and smears the targets as one. Thereby the filtered images looked quite the same regardless of the SNR value. In the case with highest noise level (signal-to-noise ratio 1.0), Ref A and the developed method were almost equally accurate.

	METHOD		
SNR	Ref A	Ref B	New
4.0	20.9	15.3	4.3
3.0	20.5	16.9	5.6
2.5	21.1	17.2	7.1
2.0	21.0	20.1	8.6
1.5	21.3	23.2	11.7
1.0	21.3	31.0	20.8

Table 1: Average errors in intensity estimates (percent)

	METHOD		
SNR	Ref A	Ref B	New
4.0	15.8	29.4	13.9
3.0	21.5	34.5	18.2
2.5	25.1	38.0	23.7
2.0	33.5	44.9	29.1
1.5	46.9	59.8	41.2
1.0	93.8	103.4	89.8

Table 2: Average errors in location estimates (nanometers).

3.3 Microscopy data

The equipment used was total internal reflection fluorescence (TIRF) microscopy Olympus IX-71 with Till imaging software and objective PLAPON TIRFM 60x/1,45. Camera sampling size was 87×87nm. HeLa cells stably expressing caveolin-1 with a C-terminal GFP tag were used. Microscope images of caveolae with fluorescent caveolin-1 protein were acquired by Institute of Biomedicine at University of Helsinki. Parameters relevant for this article were: numerical aperture $A = 1.20$, emission wavelength of the fluorophore $\lambda = 507$ nm. The data has been described more in detail in [5]. Examples of the spots from the microscope data can be seen in Figure 2.

3.4 Results with microscopy data

The results from the estimation of caveolae microscopy data can be seen in Figure 3. Based on previous studies ([1]), the single caveolae have consistent number of proteins and therefore consistent intensities in the image. The single caveolae fuse together as complexes with double or triple number of proteins, which can be observed as spots with corresponding intensities. The theoretically expected intensity distribution would thereby be such that the measured intensities form three distinct clusters. Indeed, in Figure 3 the largest cluster can be seen centred roughly at 8000, the second cluster at about 16000 and the third one approximately at 23000.

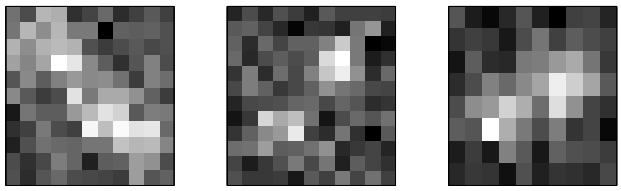

Figure 2: Examples of spots from the microscopy data.

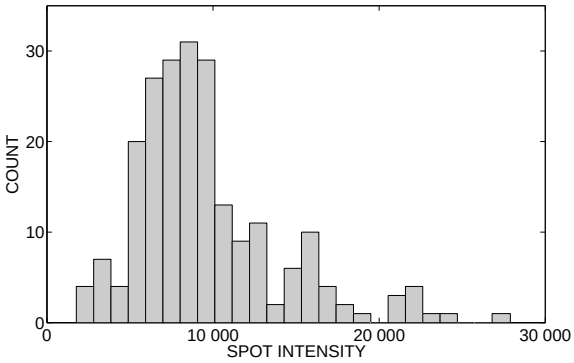

Figure 3: Histogram of estimated intensities from microscopy data

4. CONCLUSION

We have introduced a fully automatic method to quantify the spot intensities and locations from the raw microscopy images using stochastic image model and maximum likelihood estimation. In simulations the method was found to be more accurate in both spot intensity and location estimation in comparison to the reference methods. We also showed that the method is applicable to real microscopy images.

Our method can be generalized to applications, in which the target size is smaller than the camera resolution. This is the most obvious limitation in the range of applications as some prior information about the target size is required. When such information is available, we suggest using the introduced method in intensity and location determination.

5. ACKNOWLEDGEMENTS

This work was supported by the Academy of Finland, application number 129657, Finnish Programme for Centres of Excellence in Research 2006- 2011. HP received additional support from Jenny and Antti Wihuri foundation. JT received additional support from University Alliance Finland Research Cluster of Excellence STATCORE.

REFERENCES

[1] R. G. W. Anderson. The caveolae membrane system. *Annu Rev Biochem*, 67(1):199–225, July 1998.

[2] M. K. Cheezum, W. F. Walker, and W. H. Guilford. Quantitative comparison of algorithms for tracking single fluorescent particles. *Biophys. J.*, 81(4):2378–2388, October 2001.

[3] S. F. Gibson and F. Lanni. Experimental test of an analytical model of aberration in an oil-immersion objective lens used in three-dimensional light microscopy. *J. Opt. Soc. Am. A*, 9(1):154–166, 1992.

[4] R. D. Goldman and D. L. Spector. *Live cell imaging*. Natural Computing Series. CSHL Press, 2004.

[5] M. Jansen, V. M. Pietiäinen, H. Pölönen, L. Rasilainen, M. Koivusalo, U. Ruotsalainen, E. Jokitalo, and E. Ikonen. Cholesterol substitution increases the structural heterogeneity of caveolae. *J. Biol. Chem.*, page M710355200, 2008.

[6] J. Lampinen and I. Zelinka. On stagnation of the differential evolution algorithm. In *Proc. 6th International Mendel Conf. on Soft Computing*, pages 76–83, Brno, Czech Republic, June 2000.

[7] K. V. Price, R. M. Storn, and J. A. Lampinen. *Differential Evolution A Practical Approach to Global Optimization*. Natural Computing Series. Springer-Verlag, Berlin, Germany, 2007.

[8] R. Storn and K. Price. Differential evolution - a simple and efficient adaptive scheme for global optimization over continuous spaces. Technical Report TR-95-012, International Computer Science Institute, 1947 Center Street, Berkeley, CA, Berkeley, CA, 1995.

[9] D. Thomann, D. R. Rines, P. K. Sorger, and G. Danuser. Automatic fluorescent tag detection in 3d with super-resolution: application to the analysis of chromosome movement. *J Microsc*, 208(Pt 1):49–64, October 2002.